LETTER Communicated by Carson Chow

The Impact of Spike Timing Variability on the Signal-Encoding Performance of Neural Spiking Models

Amit Manwani
quixote@klab.caltech.edu
Peter N. Steinmetz
peter@klab.caltech.edu
Christof Koch
koch@klab.caltech.edu
Computation and Neural Systems, California Institute of Technology, Pasadena, CA 91125, U.S.A.

It remains unclear whether the variability of neuronal spike trains in vivo arises due to biological noise sources or represents highly precise encoding of temporally varying synaptic input signals. Determining the variability of spike timing can provide fundamental insights into the nature of strategies used in the brain to represent and transmit information in the form of discrete spike trains. In this study, we employ a signal estimation paradigm to determine how variability in spike timing affects encoding of random time-varying signals. We assess this for two types of spiking models: an integrate-and-fire model with random threshold and a more biophysically realistic stochastic ion channel model. Using the coding fraction and mutual information as information-theoretic measures, we quantify the efficacy of optimal linear decoding of random inputs from the model outputs and study the relationship between efficacy and variability in the output spike train. Our findings suggest that variability does not necessarily hinder signal decoding for the biophysically plausible encoders examined and that the functional role of spiking variability depends intimately on the nature of the encoder and the signal processing task; variability can either enhance or impede decoding performance.

1 Introduction

Deciphering the neural code remains an essential and yet elusive key to understanding how brains work. Unraveling the nature of representation of information in the brain requires an understanding of the biophysical constraints that limit the temporal precision of neural spike trains, the dominant mode of communication in the brain (Mainen and Sejnowski, 1995; van Steveninck, Lewen, Strong, Koberle, & Bialek, 1997). The representation used by the nervous system depends on the precision with which neurons

respond to their synaptic inputs (Theunissen & Miller, 1995), which in turn is influenced by noise present at the single cell level (Koch, 1999). Neuronal hardware inherently behaves in a probabilistic manner, and thus the encoding of information in the form of spike trains is noisy and may result in irregular timing of individual action potentials in response to identical inputs (Schneidman, Freedman, & Segev, 1998). As in other physical systems, noise has a direct bearing on how information is represented, transmitted, and decoded in biological information processing systems (Cecchi et al., 2000), and a quantitative understanding of neuronal noise sources and their effect on the variability of spike timing reveals the constraints under which neuronal codes must operate.

The variability of spike timing observed in vivo can arise due to a variety of factors. One possibility is that it originates at the level of the single neuron, due to either a delicate balance of the excitatory and inhibitory synaptic inputs it receives (Shadlen & Newsome, 1998) or sources of biological noise intrinsic to it (Schneidman et al., 1998). The other possibility is that variability is an emergent property of large, recurrent networks of spiking neurons connected in a certain fashion, representing faithful encoding of nonlinear or chaotic network dynamics (van Vreeswijk & Sompolinsky, 1996, 1998). Such faithful encoding argues in favor of the hypothesis that single neurons are capable of very precise signaling; high spike timing reliability is intuitively appealing since it provides a substrate for efficient temporal coding (Abeles, 1990; Bialek, Rieke, van Steveninck, & Warland, 1991; Softky & Koch, 1993).

In this study, we eschew the debate regarding the origin of variability and instead assess the functional role of spike timing variability in a specific instance of a neural coding problem: signal estimation. We quantify the ability of two types of neural spiking models, integrate-and-fire models and stochastic ion channel models, to encode information about their random time-varying inputs. The goal in signal estimation is to estimate a random time-varying current injected into a spike-encoding model from the corresponding spike train output. The efficacy of encoding is estimated by the ability to reconstruct the inputs from the output spike trains using optimal least-mean-square estimation; we use information-theoretic measures to quantify the fraction of variability in output spike train, which conveys information about the input. We have previously reported the coding fraction for the Hodgkin-Huxley dynamics for a limited number of input bandwidths (Steinmetz, Manwani, & Koch, in press); here we report the results for more biophysically realistic encoders and for a more complete range of model parameters.

2 Methods

In the following, we consider spiking models that transform continuous, time-varying input signals into sequences of action potentials or spikes

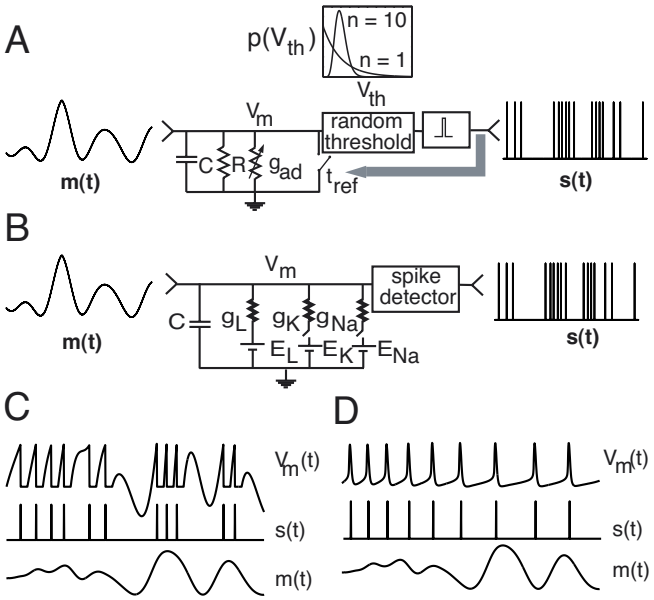

Figure 1: Noisy models of spike timing variability. (A) For an adapting integrate-and-fire model with random threshold, the time-varying input current $m(t)$ is integrated by a combination of the passive membrane resistance and capacitance (the RC circuit) to give rise to the membrane voltage V_{m}. When V_{m} exceeds a threshold V_{th} drawn from a random distribution $p(V_{\mathrm{m}})$, a spike is generated and the integrator is reset for a duration equal to the refractory period t_{ref}. The output spike train of the model in response to the input is represented as a point process $s(t)$. $p(V_{\mathrm{th}})$ is modeled as an nth-order gamma distribution where n determines the variability in spike timing (the inset shows gamma distributions for $n = 1$, 2, and 10). Each spike increases the amplitude of a conductance g_{adapt} by an amount G_{inc}. g_{adapt} corresponds to a calcium-dependent potassium conductance responsible for firing-rate adaptation and decays exponentially to zero between spikes with a time constant τ_{adapt}. (B) A time-varying current input $m(t)$ is injected into a membrane patch containing stochastic voltage-gated ion channels, which are capable of generating action potentials in response to adequately strong current inputs. When the membrane voltage exceeds an arbitrarily chosen reference value above resting potential (+10 mV, in this case), a spike is recorded in the output spike train $s(t)$. Parameters correspond to the kinetic model for regular spiking cortical neurons derived by Golomb and Amitai (1997). (C, D) Sample traces of the input $m(t)$, the membrane voltage $V_{\mathrm{m}}(t)$, and the spike train $s(t)$ for the models in *A* and *B*, respectively.

(shown in Figure 1). The spike train output of a model in response to the injection of an input current $i(t)$ is denoted by $s(t)$, which is assumed to be a point process and is mathematically modeled as a sequence of delta

functions at time instants $\{t_i\}$

$$s(t) = \sum_i \delta(t - t_i).$$

The models we consider generate irregular spike trains in response to repeated presentations of the same input and can be regarded as representations of irregular spiking behavior in real biological neurons. We use a specific signal processing task (signal estimation) to study the effects of spike timing variability on the encoding of time-varying input modulations by these models.

2.1 Measurement of Spike Timing Variability. Spike timing variability has previously been examined using two methods. The first, introduced by Mainen and Sejnowski (1995), measures the precision and reliability of spike times generated by one neuron in response to repeated presentations of the same input current. The second method, measurement of the coefficient of variation (CV) of the interspike interval distribution, examines variability of firing when a neuron is responding to natural inputs. Thus, these two measures represent two different paradigms of neuronal variability. CV is the measure used here, since determining the efficacy of information transfer during signal encoding requires the presentation of a large group of randomly selected stimuli. Although there is no general relationship between precision and reliability as measured by Mainen and Sejnowski (1995) for the encoding models examined in this study, the two measures roughly correspond, as shown in Figure 2C. We will return to this point in the Discussion.

2.2 Measurement of Coding Efficiency. In order to compute coding efficiency, we construct the optimal linear estimator of the input current $i(t)$. The difference, $m(t)$, from the mean current is a zero-mean random time-varying input signal that is encoded in the form of a spike train $s(t)$. For the purposes of this article, we assume that the current $i(t)$ injected into the model has the form $i(t) = I + m(t)$, where I is the constant component and $m(t)$ is the fluctuating component of the injected current. We assume that $m(t)$ and $s(t)$ are (real-valued) jointly weak-sense stationary (WSS) processes with finite variances, $\langle m^2(t) \rangle = \sigma_m^2 < \infty$, $\langle |s(t) - \overline{\lambda}|^2 \rangle < \infty$, where $\overline{\lambda} = \langle s(t) \rangle$ is the mean firing rate of the neuron. The operator $\langle \cdot \rangle$ denotes an average over the joint input and spike train ensemble.

The objective in signal estimation is to reconstruct the input $m(t)$ from the spike train $s(t)$ such that the mean square error (MSE) between $m(t)$ and its estimate is minimized. In general, the optimal MSE estimator is mathematically intractable to derive, so we shall restrict ourselves to the optimal linear estimator of the input (denoted by $\hat{m}(t)$), which can be written as

$$\hat{m}(t) = (g \star s)(t). \tag{2.1}$$

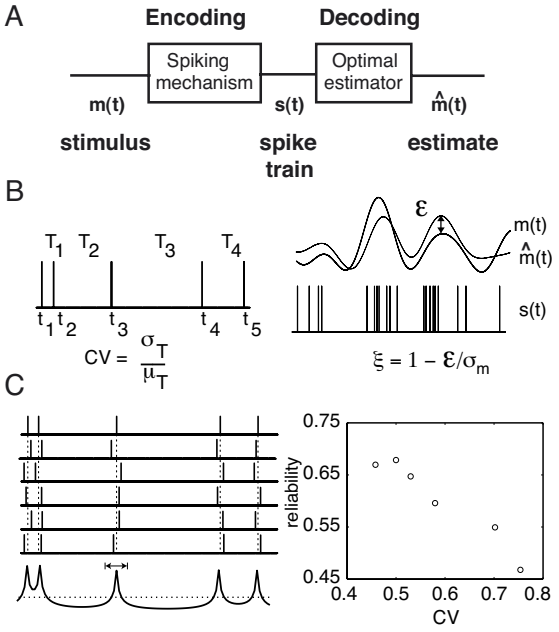

Figure 2: Block diagram of the signal estimation paradigm. (A) A noisy spike-encoding mechanism transforms a random time-varying input $m(t)$ drawn from a probability distribution into a spike train $s(t)$. Techniques from statistical estimation theory are used to derive the optimal linear estimate, $\hat{m}(t)$ of the input $m(t)$ from the spike train $s(t)$. $m(t)$ is a gaussian, band-limited, wide sense stationary (WSS) stochastic process with a power spectrum $S_{\rm mm}(f)$ that is flat over a bandwidth $B_{\rm m}$ and whose standard deviation is denoted by $\sigma_{\rm m}$. (B) Variability of the spike train is characterized by CV, the ratio of the standard deviation $\sigma_{\rm T}$ of the interspike intervals ($T_i = t_{i+1} - t_i$) to the mean interspike interval $\mu_{\rm T}$. The estimation performance is characterized by the coding fraction $\xi = 1 - \mathcal{E}/\sigma_{\rm m}$. $\mathcal{E}$ is the mean-square error between the time-varying input $m(t)$ and its optimal linear reconstruction $\hat{m}(t)$ from the spike train $s(t)$. (C) Correspondence between CV and other measures of spike irregularity. Using the procedure described in Mainen and Sejnowski (1995), reliability and precision are estimated from responses of the model to repeated presentations of the same input. The spike sequences are used to obtain the poststimulus time histogram (PSTH) shown in the lowest trace. Instances when the PSTH exceeds a chosen threshold (dotted line) are termed *events*. Reliability is defined as the fraction of spikes occurring during these events, and precision is defined as the mean length of the events. The inverse relationship between reliability and CV (as the input bandwidth is varied) validates our use of CV as a representative measure of spike variability. A similar relationship exists between precision and CV (data not shown).

The reconstruction noise $\hat{n}(t)$ for the estimation task is given as the difference between the input and the optimal estimate,

$$\hat{n}(t) = \hat{m}(t) - m(t), \tag{2.2}$$

and the reconstruction error $\mathcal{E}$ is equal to the variance of $\hat{n}(t)$, $\mathcal{E} = \langle \hat{n}^2 \rangle$. As shown in Gabbiani (1996) and Gabbiani and Koch (1996), $\hat{m}^2 \leq \hat{n}^2$ for the optimal linear estimator. Following their conventions, we define a normalized dimensionless quantity, called the *coding fraction* ξ, as follows:

$$\xi = 1 - \frac{\mathcal{E}}{\sigma_{\mathrm{m}}^2}, \qquad 0 \leq \xi \leq 1. \tag{2.3}$$

ξ can be regarded as a quantitative measure of estimation performance; $\xi = 0$ implies that the input modulations cannot be reconstructed at all, denoting estimation performance at chance, whereas $\xi = 1$ implies that the input modulations can be perfectly reconstructed.

Another measure of estimation performance is the mutual information rate, denoted by $I[m(t); s(t)]$, between the random processes $m(t)$ and $s(t)$ (Cover & Thomas, 1991). The data processing inequality (Cover & Thomas, 1991) maintains that the mutual information rate between input $m(t)$ and the spike train $s(t)$ is greater than the mutual information between $m(t)$ and its optimal estimate $\hat{m}(t)$,

$$I[m(t); s(t)] \geq I[m(t); \hat{m}(t)].$$

When the input $m(t)$ is gaussian, it can be shown (Gabbiani, 1996; Gabbiani & Koch, 1996) that $I[m(t); \hat{m}(t)]$ (and thus $I[m(t); s(t)]$) is bounded below by

$$I[m(t); \hat{m}(t)] \geq I_{\mathrm{LB}} = \frac{1}{2} \int_{-\infty}^{\infty} \mathrm{d}f \, \log_2 \left[SNR(f) \right] \quad (\text{bit sec}^{-1}), \tag{2.4}$$

where $SNR(f)$ is the signal-to-noise ratio defined as

$$SNR(f) = \frac{S_{\mathrm{mm}}(f)}{S_{\hat{\mathrm{n}}\hat{\mathrm{n}}}(f)}. \tag{2.5}$$

$S_{\mathrm{mm}}(f)$ and $S_{\hat{\mathrm{n}}\hat{\mathrm{n}}}$ are power spectral densities of the input $m(t)$ and the noise $n(t)$. In our simulations, $SNR(f)$ may be greater than one since we are separately adjusting the mean and variance of the input signal and the bandwidth of the noise. The lower bound on the information rate I_{LB} lies in the set $(0, \infty)$. The lower limit, $I_{\mathrm{LB}} = 0$, corresponds to chance performance ($\xi = 0$), whereas the upper limit, $I_{\mathrm{LB}} = \infty$, corresponds to perfect estimation ($\xi = 1$).

The information rate denotes the amount of information about the input (measured in units of bits) that can be reliably transmitted per second in

the form of spike trains. Clearly, it depends on the rate at which spikes are generated: the higher the mean firing rate, the higher is the maximum amount of information that can be transmitted per second. Thus, in order to eliminate this extrinsic dependence on mean firing rate, we define a quantity, $I_S = I_{LB}/\overline{\lambda}$, which measures the amount of information communicated per spike on average. I_S is measured in units of (bits per spike). Thus, the coding fraction (ξ) and the information rates (I_{LB}, I_S) can be used to assess the ability of the spiking models to encode time-varying inputs in the specific context of the signal estimation (Schneidmann, Segev, & Tishby, 2000).

2.3 Models of Spike Encoding. We have previously reported the coding efficiency for a noisy nonadapting integrate-and-fire model, as well as for a stochastic version of the Hodgkin-Huxley kinetic scheme (Steinmetz et al., in press). A major goal of this work was to expand this analysis to use more biophysically realistic encoders.

2.3.1 Integrate-and-Fire model. Integrate-and-fire models (I&F) are simplified, phenomenological descriptions of spiking behavior in biological neurons (Tuckwell, 1988). They retain two important aspects of neuronal firing: a subthreshold regime, where the input to the neuron is passively integrated, and a voltage threshold, which, when exceeded, leads to the generation of stereotypical spikes. Although I&F models are physiologically inaccurate, they are often used to model biological spike trains because of their analytical tractability.

Real neurons show evidence of firing-rate adaptation; their firing rate decreases with time in response to constant, steady inputs. Such adaptation can be caused by processes like the release of neurotransmitters and neuromodulators and the presence of specific ionic currents (Ca^{2+}-dependent, slow K^+) among others. Wehmeier, Dong, Koch, & van Essen (1989) introduced an I&F model with a purely time-dependent shunting conductance, g_{adapt}, with a reversal potential equal to the resting potential to account for short-term (10–50 millisecond) adaptation. Each spike increases g_{adapt} by a fixed amount G_{inc}. Between spikes, g_{adapt} decreases exponentially with a time constant τ_{adapt}. This models the effect of membrane Ca^{2+}-dependent potassium conductance, reproducing the effect of a relative refractory period following spike generation. We refer to this model as an *adapting integrate-and-fire* model. An absolute refractory period t_{ref} is required in order to mimic very short-term adaptation. In the subthreshold domain, the membrane voltage V_m is given by

$$C\frac{dV_m}{dt} + \frac{V_m(1 + R\,g_{adapt})}{R} = i(t), \tag{2.6}$$

$$\tau_{adapt}\frac{dg_{adapt}}{dt} + g_{adapt} = G_{inc}\sum_i \delta(t - t_i). \tag{2.7}$$

Table 1: Parameters for the Leaky Integrate-and-Fire Model.

$\overline{V}_{\text{th}}$	16.4 mV
C	0.207 nF
R	38.3 MΩ
t_{ref}	2.68 msec
G_{inc}	20.4 nS
τ_{adapt}	52.3 msec
Δt	0.5 msec

When V_{m} reaches the voltage threshold V_{th} at time t_i, a spike is generated if $t_i - t_{i-1} > t_{ref}$, where t_{i-1} is the time of the previous spike. When a spike is generated, $g_{\text{adapt}}(t_i)$ is also incremented by G_{inc}. The model is completely characterized by six parameters: V_{th}, C, R, t_{ref}, G_{inc}, and τ_{adapt}. The values used for our simulations are adapted from Koch (1999) and are given in Table 1.

Biological neurons in vivo show a substantial variability in the exact timing of action potentials to identical stimulus presentations (Calvin & Stevens, 1968; Softky & Koch, 1993; Shadlen & Newsome, 1998). A simple modification to reproduce the random nature of biological spike trains is to regard the voltage threshold V_{th} as a random variable drawn from some arbitrary probability distribution $p(V_{\text{th}})$ (Holden, 1976). We refer to this class as *integrate-and-fire models with random threshold*. In general, $p(V_{\text{th}})$ can be arbitrary, but here we assume that it is an nth-order gamma distribution

$$p_n(V_{\text{th}}) = c_n \left(\frac{V_{\text{th}}}{\overline{V}_{\text{th}}}\right)^{n-1} \exp\left(\frac{-nV_{\text{th}}}{\overline{V}_{\text{th}}}\right), \tag{2.8}$$

with

$$c_n = \frac{n^n}{(n-1)!}\frac{1}{\overline{V}_{\text{th}}},$$

where $\overline{V}_{\text{th}}$ denotes the mean voltage threshold. The order of the distribution, n, determines the variability of spike trains in response to the injection of a constant current. Thus, one can obtain spike trains of varying regularity by modifying n. For constant current injection and in the absence of a refractory period, the CV varies from CV = 1 to CV = 0 as n is increased from $n = 1$ to $n = \infty$ (corresponding to a deterministic threshold). A schematic diagram of the adapting I&F model with random threshold used in this article is shown in Figure 1A.

2.3.2 Stochastic Ion Channel Model. While a proper adjustment of model parameters allows I&F models to provide a fairly accurate description of

the firing properties of some cortical neurons (Stevens & Zador, 1998; Koch, 1999), many neurons cannot be modeled by I&F models. Nerve membranes contain several voltage- and ligand-gated ionic currents, which are responsible for a variety of physiological properties that phenomenological models fail to capture.

The successful elucidation of the ionic basis underlying neuronal excitability in the squid giant axon by Hodgkin and Huxley (1952) led to the development of more sophisticated mathematical models that described the initiation and propagation of action potentials by explicitly modeling the different ionic currents flowing across a neuronal membrane. In the original Hodgkin and Huxley model, membrane currents were expressed in terms of macroscopic deterministic conductances representing the selective permeabilities of the membrane to different ionic species. However, it is now known that the macroscopic currents arise as a result of the summation of stochastic microscopic currents flowing through a multitude of ion channels in the membrane.

Ion channels have been modeled as finite-state Markov chains with state transition probabilities proportional to the kinetic transition rates between different conformational states (Skaugen & Wallœ, 1979; Clay & DeFelice, 1983; Strassberg & DeFelice, 1993). In earlier research, we studied the influence of the stochastic nature of voltage-gated ion channels in excitable neuronal membranes on subthreshold membrane voltage fluctuations (Steinmetz, Manwani, Koch, London, & Segev, 2000; Manwani, Steinmetz, & Koch, 2000). Here we are interested in assessing the influence of variability in spike timing on the ability of noisy spiking mechanisms to encode time-varying inputs, in the context of stochastic ion channel models. For voltage-gated ion channels, the kinetic transition rates (and other parameters determined by them) are functions of the membrane voltage V_{m}. As in the case of the I&F model, a band-limited white noise current $m(t)$ is injected into a patch of membrane containing stochastic voltage-gated ion channels, and Monte-Carlo simulations are carried out to determine the response of the model to random suprathreshold stimuli (see Figure 1B).

The ion channel model we consider here is a stochastic counterpart of the single-compartment model of a regular-spiking cortical developed in Golomb and Amitai (1997). The original version consists of a fast sodium current, a persistent sodium current, a delayed-rectifier potassium current, an A-type potassium current (for adaptation), a slow potassium current, a passive leak current, and excitatory synaptic (AMPA- and NMDA-type) currents. We are interested in the variability due to the stochastic nature of ion channels, and so here we assume that the synaptic currents are absent. In order to simulate stochastic Markov models of the ion channel kinetics associated with five voltage-dependent ionic currents, we performed Monte Carlo simulations of single-compartmental models of membrane patches of area A. The Markov models correspond to equations A1 through A20 of Golomb and Amitai (1997) and were constructed using methods given in

Table 2: Parameters for the Stochastic Ion Channel Model.

Na^+current (I_{Na})	2 states for h
$\overline{g}_{Na}$	0.24 nS/μ^2
γ_{Na}	0.18 pS
Persistent Na^+current (I_{NaP})	Deterministic
Delayed rectifier K^+current (I_{Kdr})	5 states for n
$\overline{g}_{Kdr}$	0.24 nS/μ^2
γ_{Kdr}	0.21 pS
A-type K^+current (I_{KA})	2 states for b
$\overline{g}_{KA}$	0.24 nS/μ^2
γ_{KA}	0.020 pS
Slow K^+current (I_{K-slow})	2 states for z
$\overline{g}_{Ksl}$	0.24 nS/μ^2
γ_{Ksl}	0.20 pS
Leakage current (I_L)	Deterministic

Skaugen and Wallœ (1979), Skaugen (1980), and Steinmetz et al. (2000). The particular parameters used for these simulations are given in Table 2.

We chose a sufficiently small time step for the simulation so that the membrane voltage can be assumed to be relatively constant over the duration of the step. The voltage-dependent state transition probabilities are computed for each time step.[1] Knowledge of the transition probabilities between states is used to determine the modified channel populations occupying different states. This is done by drawing random numbers specifying the number of channels making transitions between any two states from multinomial distributions parameterized by the transition probabilities. The membrane conductance due to a specific ion channel is determined by tracking the number of members of the given channel type that are in its open state. This membrane current is integrated over the time step to compute the membrane voltage for the next time step. This procedure is applied iteratively to obtain the membrane voltage trajectory in response to the input current waveform. For a detailed description of the Monte Carlo simulations, see Schneidman et al. (1998) and Steinmetz et al. (2000).

The voltage trajectory is transformed into a point process by considering the instance of the voltage crossing a threshold (here, 10 mV with respect to resting potential) as a spike occurrence. Thresholding allows us to treat the output of the model as a sequence of spike times rather than as membrane voltage modulations. This simple recipe to detect spikes works well for the model we consider here.

[1] The transition probabilities are computed by multiplying the corresponding rates by the length of the time step, assuming the product is much smaller than one.

3 Results

We carried out simulations for the I&F model and the stochastic ion channel model and recorded the output spike times in response to the injection of a current equal to a mean current, I, plus pseudo-random, gaussian, band-limited noise (flat power spectrum $S_{\mathrm{mm}}(f)$ over bandwidth B_{m}) ($f \in (0, B_{\mathrm{m}}]$). We then computed the CV of the interspike interval distribution and the coding fraction, ξ, for signal estimation task. CV measures the variability of the spike train in response to the input, whereas the coding fraction quantifies the fraction of the variability in the spike train, which is functionally useful to reconstruct the input modulations. Once again, our goal is to understand how spike timing variability influences performance in a specific biological information processing task—here, a signal estimation task.

3.1 Dependence of Variability on Firing Rate and Bandwidth. First, we explored the dependence of the coefficient of variability of the interspike interval, CV, on the mean firing rate $\overline{\lambda}$ of the spiking models. Figure 3A shows the CV as a function of $\overline{\lambda}$ for an input bandwidth of B_{m}= 50 Hz. The mean firing rate $\overline{\lambda}$ for the I&F model depends on only the mean injected current I, whereas for membrane patch–containing stochastic ion channels, $\overline{\lambda}$ depends on a variety of additional parameters, such as the area of the patch A, the standard deviation of the stochastic input noise current σ_{m}, and bandwidth of the input B_{m}. For both models, we varied $\overline{\lambda}$ while maintaining the contrast of the input, defined as $c = \sigma_{\mathrm{m}}/I$, constant at $c = 1/3$. In both cases, CV increased monotonically with mean firing rate. When the contrast is kept constant, an increase in I (to increase the mean firing rate) requires a corresponding increase in the magnitude of the fluctuations σ_{m}. This results in an increase in the amplitude of firing-rate modulations, allowing the input to be estimated more accurately.

Figure 3B shows the CV for the two models as a function of the bandwidth of the input B_{m}. For both models, total noise power was held constant at all bandwidths, and I was adjusted so that the mean firing rate $\overline{\lambda}$ was approximately equal to 50 Hz. In both cases, CV decreases with increasing B_{m}, which is in qualitative agreement with earlier experimental (Mainen & Sejnowski, 1995) and computational (Schneidman et al., 1998) findings demonstrating an inverse relationship between spike timing precision (using a measure different from CV) and the temporal bandwidth of the input. Strong temporal dynamics in the input to a neuron dwarf the effect of the inherent noise in the spiking mechanism and regularize the spike train. Within the class of I&F models, models with higher n fire more regularly and have lower CV values, as expected.

3.2 Dependence of Encoding Performance on Firing Rate and Bandwidth. Next, we explored the dependence of coding efficiency on the mean

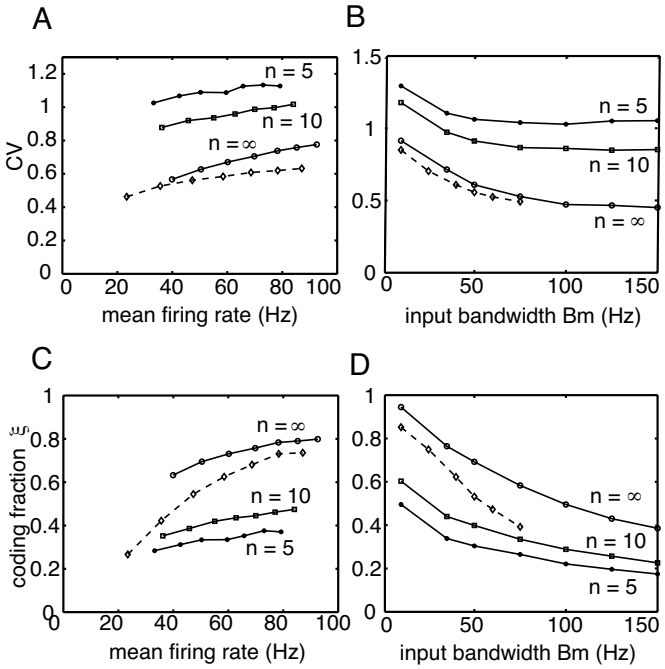

Figure 3: Variability and coding efficiency of spiking models. (A) CV of the interspike interval distribution of the spike train as a function of the mean firing rate of the spike train $\overline{\lambda}$. The input to the model is a gaussian, white, band-limited (bandwidth B_{m} = 50 Hz) input, with mean I and standard deviation σ_{m}. The mean firing rate of the model is varied by changing the mean current I while maintaining the contrast of the input, defined as $c = \sigma_{\mathrm{m}}/I$, constant (c = 1/3). The solid curves correspond to the adapting I&F model for different values of the order n of the gamma-distributed voltage threshold distribution ($n = \infty$ corresponds to a deterministic threshold). The dotted curve corresponds to a 1000 μm^2 membrane patch containing stochastic ion channels. (B) CV as a function of input bandwidth B_{m}. $\overline{\lambda}$ for both the models was maintained at 50 Hz. (C, D) The dependence of the coding fraction ξ in the signal estimation task for the two types of spiking models on the mean firing rate $\overline{\lambda}$ (for B_{m} = 50 Hz) and the input bandwidth B_{m} (for $\overline{\lambda}$ = 50 Hz), respectively. Model parameters are summarized in the caption of Figure 1.

firing rate and the input bandwidth. In Figures 3C and 3D, the coding fraction ξ is plotted as a function of $\overline{\lambda}$ (for B_m = 50 Hz) and B_{m} ($\overline{\lambda}$ = 50 Hz), respectively. For both spike-encoding mechanisms, ξ increases with mean

firing rate and decreases with input bandwidth. One interpretation of the previously observed decrease in variability of spike timing with input bandwidth (see Figure 3B) is that it suggests an improvement in coding—that in a sense, the neuron prefers higher bandwidths (Schneidman, Freedman, & Segev, 1997). By contrast, we find that the noisy spike-encoding models considered here encode slowly varying stimuli more effectively than rapid ones. We believe that in the context of a signal estimation task, this is a generic property of all models that encode continuous signals as firing-rate modulations of sequences of discrete spike trains.

3.3 Dependence of Mutual Information on Firing Rate and Bandwidth. Next, we explored the dependence of the mutual information rates on the mean firing rate and input bandwidth. Figures 4A and 4B, respectively, show that the lower bound of the mutual information rate I_{LB} increases with $\overline{\lambda}$ and B_{m}. This behavior can be better understood in the light of the phenomenological expression $I_{\mathrm{LB}} = B_{\mathrm{m}} \log_2(1 + \kappa\,\overline{\lambda}/B_{\mathrm{m}})$, where κ is a constant that depends on the details of the encoding scheme. The above expression is exact when the instantaneous firing rate of the model is a linear function of the input (as in the case of the perfect I&F model) and the input is a white band-limited gaussian signal with bandwidth B_{m}. For a Poisson model without adaptation, $\kappa = c^2/2$. (Details of the derivation of this expression are provided in Manwani and Koch, 2001.) From the above expression, one can deduce that for low firing rates, I_{LB} increases linearly with $\overline{\lambda}$, but at higher rates, I_{LB} becomes logarithmic with $\overline{\lambda}$. One can also conclude that I_{LB} increases with B_{m} for small bandwidths but quickly saturates at high bandwidths at the value $\kappa\overline{\lambda}/\ln 2$. This qualitatively agrees with Figures 4A and 4B.

The dependence of the information rate per spike I_{S} on $\overline{\lambda}$ and B_{m} can be similarly explored. The expression for I_{LB} is sublinear with respect to $\overline{\lambda}$, and thus one can deduce that I_{S} should decrease monotonically with firing rate when the bandwidth B_{m} is held fixed. In fact, its maximum value, $I_{\mathrm{S}} = \kappa$, occurs at $\overline{\lambda} = 0$. On the other hand, when $\overline{\lambda}$ is held fixed, I_{S} should increase with B_{m} initially but saturate at high bandwidths at $\kappa/\ln 2$. Once again, Figures 4C and 4D agree qualitatively with these predictions.

3.4 Relationship Between Variability and Encoding Performance. In order to understand further the role of variability in the context of signal estimation, we plot measures of coding efficiency (ξ and $I_{\mathrm{LB}}/B_{\mathrm{m}}$) versus the corresponding CV values for the two models as different parameters are varied. Figures 5A and 5B show the dependence of coding performance on the variability of spike timing for the I&F model, and Figures 5C and 5D show the corresponding behaviors for the stochastic ion channel model. For both models, estimation performance improves with variability when the mean firing rate was increased or the input bandwidth was decreased. This implies that the variability in the output spike train rep-

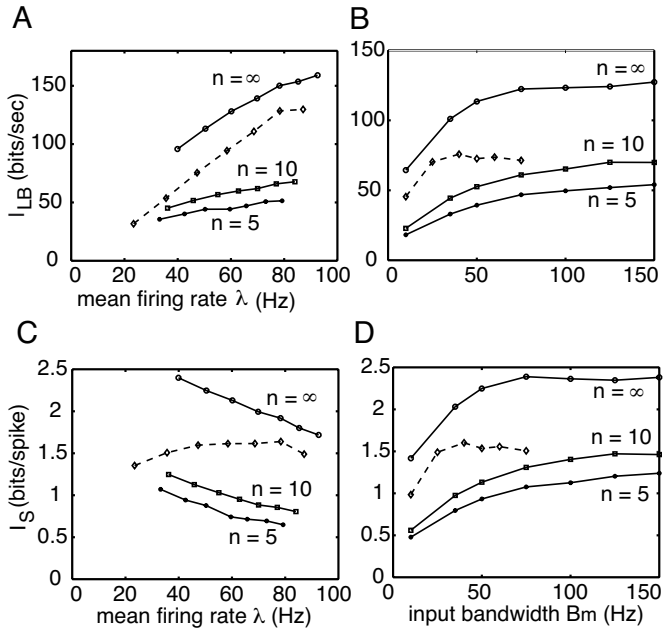

Figure 4: Information rates in signal estimation for spiking models. (A) Lower bounds of the information rate I_{LB} for the two spiking model classes considered in this article. The solid curves correspond to the adapting I&F model for different values of n, and the dotted curve corresponds to the stochastic ion channel model. As in Figure 3, the input is a band-limited gaussian process with bandwidth B_{m} = 50 Hz. (B) I_{LB} as a function of the input bandwidth B_{m} for $\overline{\lambda}$ = 50 Hz. (C) The mutual information transmitted per spike on average, $I_{\mathrm{S}} = I_{\mathrm{LB}}/\overline{\lambda}$, as a function of $\overline{\lambda}$ (B_{m} = 50 Hz). (D) I_{S} as a function of input bandwidth B_{m} for $\overline{\lambda}$ = 50 Hz. Model parameters are summarized in the caption of Figure 1.

resents faithful encoding of the input modulations, and thus greater variability leads to better signal estimation. On the other hand, when either the order of the gamma distribution for the I&F model or the area of the membrane patch for the stochastic ion channel model was decreased, coding performance decreased with variability. This suggests that the variability is due to noise (randomness of the spiking threshold). Thus, we find that the effect of spike timing variability on the coding efficiency of spiking models may be beneficial or detrimental; the direction of its influence depends on the specific nature of the signal processing task the neuron is expected to perform (signal estimation here) and the parameter that is varied.

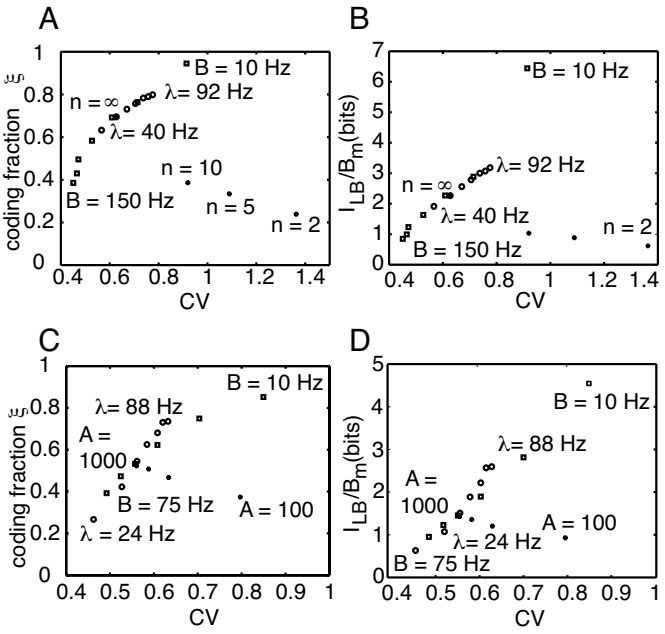

Figure 5: Is it signal or is it noise? Parametric relationships between measures of coding efficiency and the variability of the spike train as different parameters were varied for the two spiking models. (A) Coding fraction ξ and (B) mutual information transmitted per input time constant I_{LB}/B_m for the I&F model as a function of the CV of the spike train. Squares plot results while input bandwidth was varied between 10 and 150 Hz. Open circles plot results while the mean input was varied to change the firing rate from 40 to 92 Hz. Filled circles show results for the order of the gamma distribution of thresholds varied from 2 to infinity. The increase in estimation performance with CV when the mean firing rate $\overline{\lambda}$ was increased or the input bandwidth B_m was decreased (with $n = \infty$ for the I&F model) suggests that the variability arises as a result of faithful encoding of the input and thus represents signal, whereas a decrease with CV when the order n of the threshold distribution was decreased suggests that the variability impedes encoding and thus represents noise. (C) Coding fraction ξ and (D) mutual information transmitted per input time constant I_{LB}/B_m for the stochastic ion channel model as a function of the CV of the spike train as the mean firing rate $\overline{\lambda}$ (A = 1000 μm^2, B_m = 50 Hz, open circles), input bandwidth B_m (A = 1000 μm^2, $\overline{\lambda}$ = 50 Hz, open squares), and the area of the patch A (B_m = 50 Hz, $\overline{\lambda}$ = 50 Hz, filled circles) were varied.

3.5 Mean Rate Code in Signal Estimation. Figures 6A and 6B demonstrate that for the spiking models we have considered here, performance in the signal estimation task is determined by the ratio $\overline{\lambda}/B_m$ and not by

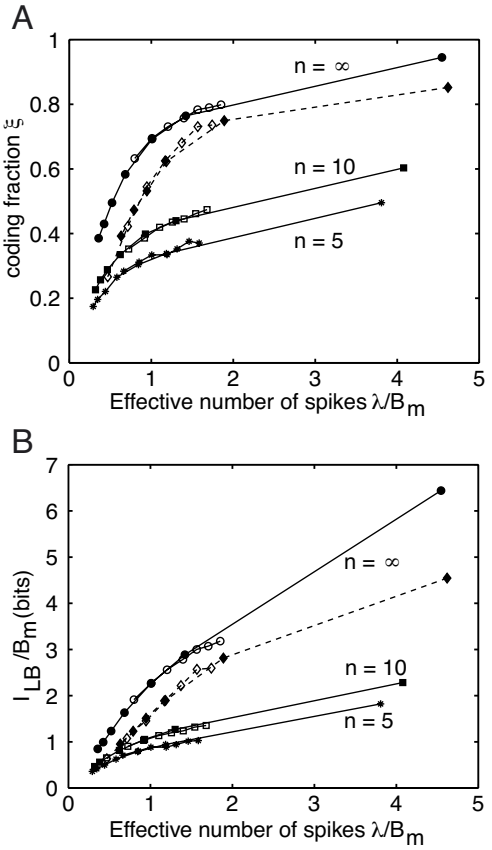

Figure 6: Coding efficiency as a function of $\overline{\lambda}/B_{\mathrm{m}}$. (A) Coding fraction ξ and (B) mutual information transmitted per input time constant, $I_{\mathrm{LB}}/B_{\mathrm{m}}$, for the two spiking models as a function of the mean number of spikes available per input time constant, $\overline{\lambda}/B_{\mathrm{m}}$, for different combinations of B_{m} and $\overline{\lambda}$ (empty symbols: B_m varied, empty symbols: $\overline{\lambda}$ varied). The solid curves correspond to the adapting I&F model (different symbols represent different values of the order, n, of the voltage threshold gamma distribution), whereas the dotted curve corresponds to a 1000 μm^2 membrane patch containing stochastic ion channels. The contrast of the input, c, was maintained at one-third.

the absolute values of $\overline{\lambda}$ and B_{m}. The quantity $\overline{\lambda}/B_{\mathrm{m}}$ represents the number of spikes observed during an input time constant, a time interval over which the input is relatively constant. Thus, the larger the number of spikes available for the estimation task, the better the estimate of the neuron's instantaneous firing rate $\lambda(t)$ and, consequently, the better the estimate of

the instantaneous value of the input $m(t)$. This suggests that the relevant variable that encodes the input modulations is the neuron's (instantaneous) firing rate computed over time intervals of length $1/B_{\mathrm{m}}$. Furthermore, the more action potential per time constant of encoding, the more efficient information can be estimated using mean rate codes.

4 Discussion

In this article, we use two types of noisy spiking models to study the influence of spike timing variability on the ability of single neurons to encode time-varying signals in their output spike trains. Here we extend the preliminary results for simplified channel models reported previously (Steinmetz et al., in press) to more biophysically realistic models of spike encoding. For both I&F models with noisy thresholds and stochastic ion channel encoders, we find that decreased spike timing variability, as assayed using the CV of the interspike interval distribution, does not necessarily translate to an increase in performance for all signal processing tasks. These results show that although the variability of spike timing decreases for these encoders as the bandwidth of the input is increased, the ability to estimate random continuous signals drops. Conversely, an increase in variability with firing rate also causes an increase in estimation performance.

A similar connection between increased variability and increased signal detection performance is observed in systems that exhibit stochastic resonance (Chialvo, Dykman, & Millonas, 1995; Chialvo, Longtin, & Muller-Gerking, 1997; Collins, Chow, & Imhoff, 1995a, 1995b; Henry, 1999; Russell, Wilkens, & Moss, 1999). In these systems, the addition of noise both increases output variability and improves signal transduction. In the encoding models studied here, noise is added by the stochastic nature of the ion channels responsible for action potential production, which could evoke stochastic resonance for specific encoding tasks. For hippocampal CA1 cells, the addition of synaptic noise has recently been shown to evoke stochastic resonance when detecting periodic pulse trains (Stacey & Durand, 2000).

The observed trends of CV as a function of firing rate (cf. Figure 3) are in agreement with those previously reported (Christodoulou & Bugmann, 2000; Tiesinga, Jose, & Sejnowski, 2000) and correspond to an encoder driven by Gaussian noise, but not to a system driven by a Poisson process (Tiesinga et al., 2000). We have previously shown that for subthreshold voltages, noise generated by stochastic channel models is well approximated by a gaussian distribution (Steinmetz et al., 2000); thus, the combination of these observations suggests that a gaussian distribution may function as a good approximation for suprathreshold effects as well.

The trends of coding fraction as a function of input bandwidth are also in qualitative agreement with experimental measurements of the coding fraction in cortical pyramidal cells reported by Fellous et al. (2001), although

there are differences in the input signal, which was sinusoidal for these experiments.

While interpreting these results, a few limitations must be borne in mind. We measure coding performance for gaussian, white band-limited inputs in the context of a specific signal estimation paradigm. Generally, the computation performed by real neurons in the brain and the statistical properties of the milieu of signals in which they operate are difficult to determine. Estimation performance using white noise does not shed light on the operation of neural systems highly specialized to detect specific input patterns or those optimized to process natural and ecologically relevant signals with specific statistical properties. However, in the absence of knowledge regarding the role of a single neuron, the coding fraction for white noise stimuli represents a convenient metric to quantify its behavior.

The second general limitation is that we employ simple linear decoding to recover the input from the spike train, which is inferior in performance to general nonlinear decoding mechanisms. However, it has been argued that when the mean rate or some function of it is the relevant encoding variable, the difference in performance between linear and nonlinear estimators is marginal (Rieke, Warland, van Steveninck, & Bialek, 1997) and the coding fraction is a good indicator of coding efficiency.

Finally, this study assumes that information is encoded at the level of single neurons. The investigation of the role of variability on the ability of a population of neurons to encode information is a significantly more complicated and interesting problem since temporal synchrony between groups of neurons in a population may enhance or decrease coding efficiency. We are currently investigating this issue.

Earlier studies have shown that neurons fire more predictably and precisely when their inputs have richer temporal structure (Mainen & Sejnowski, 1995; Schneidman et al., 1998). It has also been argued that the ability to alter the accuracy of their representation depending on the nature of their inputs may enable neurons to adapt to the statistical structure of their ecological environment and act as "smart encoders" (Schneidman et al., 1998; Brenner, Rieke, & de Ruyter van Steveninck, 2000; Cecchi et al., 2000). One example would be using a coarse rate code to encode slowly varying input signals but a fine temporal code to encode rapidly varying inputs.

While we agree with the basic premise of the argument, viewing variability from a different paradigm, namely signal estimation, and assaying variability with CV, suggests that variability could represent the input signal in biophysically plausible encoders; thus, encoding efficiency increases with increasing variability for several of the encoders examined here. For those encoders, spike timing reliability decreases with increasing CV, as shown in Figure 2, so in these cases, reliability will be decreasing as coding efficiency increases, providing one counterexample wherein an increase in reliability does not lead to better performance in a signal reconstruction

task. This leads us to argue that the role of variability depends intimately on the nature of the information processing task and the nature of the spike encoder. These results also highlight the need to further measure and understand biophysical noise sources and the mechanisms of computation in cortical neurons.

Acknowledgments

This work was funded by the NSF Center for Neuromorphic Systems Engineering at Caltech, the NIMH, and the Sloan-Swartz Center for Theoretical Neuroscience. We thank Idan Segev, Michael London, and Elad Schneidman for their invaluable suggestions.

References

Abeles, M. (1990). *Corticonics: Neural circuits of the cerebral cortex*. Cambridge: Cambridge University Press.

Bialek, W., Rieke, F., van Steveninck, R. R. D., & Warland, D. (1991). Reading a neural code. *Science, 252*, 1854–1857.

Brenner, N., Bialek, W., & de Ruyter van Steveninck, R. (2000). Adaptive rescaling maximizes information transmission. *Neuron, 26*, 695–702.

Calvin, W. H., & Stevens, C. F. (1968). Synaptic noise and other sources of randomness in motoneuron interspike intervals. *J. Neurophysiol., 31*, 574–587.

Cecchi, G. A., Mariano, S., Alonso, J. M., Martinez, L., Chialvo, D. R., & Magnasco, M. O. (2000). Noise in neurons is message-dependent. *PNAS, 97*(10), 5557–5561.

Chialvo, D. R., Dykman, M. I., & Millonas, M. M. (1995). Fluctuation-induced transport in a periodic potential: Noise versus chaos. *Physical Review Letters, 78*(8), 1605.

Chialvo, D. R., Longtin, A., & Muller-Gerking, J. (1997). Stochastic resonance in models of neuronal ensembles. *Physical Review E, 55*(2), 1798–1808.

Christodoulou, C., & Bugmann, G. (2000). Near Poisson-type firing produced by concurrent excitation and inhibition. *Biosystems, 58*, 41–48.

Clay, J. R., & DeFelice, L. J. (1983). Relationship between membrane excitability and single channel open-close kinetics. *Biophys. J., 42*, 151–157.

Collins, J. J., Chow, C. C., & Imhoff, T. T. (1995a). Aperiodic stochastic resonance in excitable systems. *Physical Review. E. Statistical Physics, Plasmas, Fluids, and Related Interdisciplinary Topics, 52*(4), R3321–R3324.

Collins, J. J., Chow, C. C., & Imhoff, T. T. (1995b). Stochastic resonance without tuning. *Nature, 376*(6537), 236–238.

Cover, T. M., & Thomas, J. A. (1991). *Elements of information theory*. New York: Wiley.

Fellous, J. M., Houweling, A. R., Modi, R. H., Rao, R. P. N., Tiesinga, P. H. E., & Sejnowski, T. J. (2001). Frequency dependence of spike timing reliability in cortical pyramidal cells and interneurons. *Journal of Neurophysiology, 85*, 1782–2001.

Gabbiani, F. (1996). Coding of time-varying signals in spike trains of linear and half-wave rectifying neurons. *Network: Comput. Neural Syst., 7*, 61–85.

Gabbiani, F., & Koch, C. (1996). Coding of time-varying signals in spike trains of integrate-and-fire neurons with random threshold. *Neural Comput., 8*, 44–66.

Golomb, D., & Amitai, Y. (1997). Propagating neuronal discharges in neocortical slices: Computational and experimental study. *J. Neurophysiol., 78*, 1199–1211.

Henry, K. R. (1999). Noise improves transfer of near-threshold, phase-locked activity of the cochlear nerve: Evidence for stochastic resonance? *J. Comp. Physiol. (A), 184*(6), 577–584.

Hodgkin, A. L., & Huxley, A. F. (1952). A quantitative description of membrane current and its application to conductation and excitation in nerve. *J. Physiol. (Lond.), 117*, 500–544.

Holden, A. V. (1976). *Models of the stochastic activity of neurones*. New York: Springer-Verlag.

Koch, C. (1999). *Biophysics of computation: Information processing in single neurons*. New York: Oxford University Press.

Mainen, Z. F., & Sejnowski, T. J. (1995). Reliability of spike timing in neocortical neurons. *Science, 268*, 1503–1506.

Manwani, A., & Koch, C. (2001). Detecting and estimating signals over noisy and unreliable synapses: Information-theoretic analysis. *Neural Comput., 13*, 1–33.

Manwani, A., Steinmetz, P. N., & Koch, C. (2000). Channel noise in excitable neuronal membranes. In S. A. Solla, T. K. Leen, & K.-R. Müller (Eds.), *Advances in neural information processing systems, 12* (pp. 143–149). Cambridge, MA: MIT Press.

Rieke, F., Warland, D., van Steveninck, R. D. R., & Bialek, W. (1997). *Spikes: Exploring the neural code*. Cambridge, MA: MIT Press.

Russell, D. F., Wilkens, L. A., & Moss, F. (1999). Use of behavioural stochastic resonance by paddle fish for feeding. *Nature, 402*(6759), 291–294.

Schneidman, E., Freedman, B., & Segev, I. (1997). Ion-channel stochasticity may be a critical factor in determining the reliability of spike timing. *Neurosci-L Supplement, 48*, 543–544.

Schneidman, E., Freedman, B., & Segev, I. (1998). Ion-channel stochasticity may be critical in determining the reliability and precision of spike timing. *Neural Comput., 10*, 1679–1703.

Schneidmann, E., Segev, I., & Tishby, N. A. (2000). Information capacity and robustness of stochastic neuron models. In S. A. Solla, T. K. Leen, & K.-R. Müller (Eds.), *Advances in neural information processing systems, 12*. Cambridge, MA: MIT Press.

Shadlen, M. N., & Newsome, W. T. (1998). The variable discharge of cortical neurons: Implications for connectivity, computation, and information coding. *J. Neurosci., 18*, 3870–3896.

Skaugen, E. (1980). Firing behavior in stochastic nerve membrane models with different pore densities. *Acta Physiol. Scand., 108*, 49–60.

Skaugen, E., & Wallœ, L. (1979). Firing behavior in a stochastic nerve membrane model based upon the Hodgkin-Huxley equations. *Acta Physiol. Scand., 107*, 343–363.

Softky, W. R., & Koch, C. (1993). The highly irregular firing of cortical cells is inconsistent with temporal integration of random EPSPS. *J. Neurosci., 13*, 334–350.

Stacey, W. C., & Durand, D. M. (2000). Stochastic resonance improves signal detection in hippocampal CA1 neurons. *J. Neurophysiol., 83*(3), 1394–1402.

Steinmetz, P. N., Manwani, A., & Koch, C. (in press). Variability and coding efficiency of noisy neural spike encoders. *Biosystems*.

Steinmetz, P. N., Manwani, A., Koch, C., London, M., & Segev, I. (2000). Subthreshold voltage noise due to channel fluctuations in active neuronal membranes. *J. Comput. Neurosci., 9*, 133–148.

Stevens, C. F., & Zador, A. M. (1998). Novel integrate-and-fire-like model of repetitive firing in cortical neurons. In: *Proceedings of the 5th Joint Symposium on Neural Computation* (La Jolla, CA).

Strassberg, A. F., & DeFelice, L. J. (1993). Limitations of the Hodgkin-Huxley formalism: Effect of single channel kinetics on transmembrane voltage dynamics. *Neural Comput., 5*, 843–855.

Theunissen, F., & Miller, J. P. (1995). Temporal encoding in nervous systems: A rigorous definition. *J. Comput. Neurosci., 2*, 149–162.

Tiesinga, P. H. E., Jose, J. V., & Sejnowski, T. J. (2000). Comparison of current-driven and conductance-driven neocortical model neurons with Hodgkin-Huxley voltage-gaged channels. *Physical Review E, 62*(6), 8413–8419.

Tuckwell, H. C. (1988). *Introduction to theoretical neurobiology II: Nonlinear and stochastic theories*. Cambridge: Cambridge University Press.

van Steveninck, R. R. D., Lewen, G. D., Strong, S. P., Koberle, R., & Bialek, W. (1997). Reproducibility and variability in neural spike trains. *Science, 275*, 1805–1808.

van Vreeswijk, C., & Sompolinsky, H. (1996). Chaos in neuronal networks with balanced excitatory and inhibitory activity. *Science, 274*(5293), 1724–1726.

van Vreeswijk, C., & Sompolinsky, H. (1998). Chaotic balanced state in a model of cortical circuits. *Neural Comput., 10*, 1321–1371.

Wehmeier, U., Dong, D., Koch, C., & van Essen, D. (1989). Modeling the mammalian visual system. In C. Koch & I. Segev (Eds.), *Methods in neuronal modeling*. Cambridge, MA: MIT Press.

Received June 20, 2000; accepted May 2, 2001.